The Meteoritical Society

Meteoritics & Planetary Science 49, Nr 9, 1548–1561 (2014)
doi: 10.1111/maps.12125

Stardust Interstellar Preliminary Examination III: Infrared spectroscopic analysis of interstellar dust candidates

Hans A. BECHTEL[1]*, George J. FLYNN[2], Carlton ALLEN[3], David ANDERSON[4], Asna ANSARI[5], Saša BAJT[6], Ron K. BASTIEN[7], Nabil BASSIM[8], Janet BORG[9], Frank E. BRENKER[10], John BRIDGES[11], Donald E. BROWNLEE[12], Mark BURCHELL[13], Manfred BURGHAMMER[14], Anna L. BUTTERWORTH[4], Hitesh CHANGELA[15], Peter CLOETENS[14], Andrew M. DAVIS[16], Ryan DOLL[17], Christine FLOSS[17], David R. FRANK[7], Zack GAINSFORTH[4], Eberhard GRÜN[18], Philipp R. HECK[5], Jon K. HILLIER[19], Peter HOPPE[20], Bruce HUDSON[21], Joachim HUTH[20], Brit HVIDE[5], Anton KEARSLEY[22], Ashley J. KING[5,16], Barry LAI[23], Jan LEITNER[20], Laurence LEMELLE[24], Hugues LEROUX[25], Ariel LEONARD[17], Robert LETTIERI[4], William MARCHANT[4], Larry R. NITTLER[26], Ryan OGLIORE[27], Wei Ja ONG[17], Frank POSTBERG[19,28], Mark C. PRICE[13], Scott A. SANDFORD[29], Juan-Angel Sans TRESSERAS[14], Sylvia SCHMITZ[10], Tom SCHOONJANS[30], Geert SILVERSMIT[30], Alexandre S. SIMIONOVICI[31], Vicente A. SOLÉ[14], Ralf SRAMA[28], Frank J. STADERMANN[17], Thomas STEPHAN[16], Veerle J. STERKEN[18,28,32], Julien STODOLNA[4], Rhonda M. STROUD[8], Steven SUTTON[23], Mario TRIELOFF[19], Peter TSOU[33], Akira TSUCHIYAMA[34], Tolek TYLISZCZAK[1], Bart VEKEMANS[30], Laszlo VINCZE[30], Joshua Von KORFF[4], Andrew J. WESTPHAL[4], Naomi WORDSWORTH[35], Daniel ZEVIN[4], Michael E. ZOLENSKY[3], and >30,000 Stardust@home dusters[36]

[1]Advanced Light Source, Lawrence Berkeley National Laboratory, Berkeley, California, USA
[2]SUNY Plattsburgh, Plattsburgh, New York, USA
[3]ARES, NASA Johnson Space Center, Houston, Texas, USA
[4]Space Sciences Laboratory, U.C. Berkeley, Berkeley, California, USA
[5]Robert A. Pritzker Center for Meteoritics and Polar Studies, The Field Museum of Natural History, Chicago, Illinois, USA
[6]DESY, Hamburg, Germany
[7]ESCG, NASA Johnson Space Center, Houston, Texas, USA
[8]Materials Science and Technology Division Naval Research Laboratory, Washington, District of Columbia, USA
[9]IAS Orsay, Orsay, France
[10]Geoscience Institute, Goethe University Frankfurt, Frankfurt, Germany
[11]Space Research Centre, University of Leicester, Leicester, UK
[12]Department of Astronomy, University of Washington, Seattle, Washington, USA
[13]University of Kent, Canterbury, Kent, UK
[14]European Synchrotron Radiation Facility, Grenoble, France
[15]George Washington University, Washington, District of Columbia, USA
[16]University of Chicago, Chicago, Illinois, USA
[17]Washington University, St. Louis, Missouri, USA
[18]Max-Planck-Institut für Kernphysik, Heidelberg, Germany
[19]Institut für Geowissenschaften, Universitat Heidelberg, Heidelberg, Germany
[20]Max-Planck-Institut für Chemie, Mainz, Germany
[21]Ontario, Canada
[22]Natural History Museum, London, UK
[23]Advanced Photon Source, Argonne National Laboratory, Chicago, Illinois, USA
[24]Ecole Normale Superieure de Lyon, Lyon, France
[25]University Lille 1, Lille 1, France
[26]Carnegie Institution of Washington, Washington, District of Columbia, USA

[27]University of Hawai'i at Manoa, Honolulu, Hawai'i, USA
[28]Institut für Raumfahrtsysteme, Universität Stuttgart, Germany
[29]NASA Ames Research Center, Moffett Field, California, USA
[30]University of Ghent, Ghent, Belgium
[31]Institut des Sciences de la Terre, Observatoire des Sciences de l'Univers de Grenoble, Grenoble, France
[32]Institut für Geophysik und Extraterrestrische Physik, TU Braunschweig, Braunschweig, Germany
[33]Jet Propulsion Laboratory, Pasadena, California, USA
[34]Osaka Univerisity, Osaka, Japan
[35]South Buckinghamshire, UK
[36]Worldwide
*Corresponding author. E-mail: habechtel@lbl.gov

(Received 06 December 2012; revision accepted 15 April 2013)

Abstract–Under the auspices of the Stardust Interstellar Preliminary Examination, picokeystones extracted from the Stardust Interstellar Dust Collector were examined with synchrotron Fourier transform infrared (FTIR) microscopy to establish whether they contained extraterrestrial organic material. The picokeystones were found to be contaminated with varying concentrations and speciation of organics in the native aerogel, which hindered the search for organics in the interstellar dust candidates. Furthermore, examination of the picokeystones prior to and post X-ray microprobe analyses yielded evidence of beam damage in the form of organic deposition or modification, particularly with hard X-ray synchrotron X-ray fluorescence. From these results, it is clear that considerable care must be taken to interpret any organics that might be in interstellar dust particles. For the interstellar candidates examined thus far, however, there is no clear evidence of extraterrestrial organics associated with the track and/or terminal particles. However, we detected organic matter associated with the terminal particle in Track 37, likely a secondary impact from the Al-deck of the sample return capsule, demonstrating the ability of synchrotron FTIR to detect organic matter in small particles within picokeystones from the Stardust interstellar dust collector.

INTRODUCTION

Interstellar dust grains are found throughout the interstellar medium and play a central role in molecule formation and the dynamics of star creation. Although dust accounts for only a small fraction of the baryonic mass in the Universe, it is estimated that at least 30% of the light emitted by stars is absorbed by interstellar dust and then reradiated in the infrared (Bernstein et al. 2002; Draine 2003). Consequently, much of what is known about interstellar dust has been determined from astronomical infrared spectroscopy. These measurements show that interstellar dust has a strong, broad emission feature near 10 μm, consistent with amorphous silicates (Draine 2003; Henning 2010), and several weaker features near 3.4 μm, consistent with aliphatic $–CH_2$ and $–CH_3$ stretching absorptions (Sandford et al. 1991; Whittet et al. 1997). Astronomical measurements, however, have not been able to determine the specific carriers of these emission features.

NASA's Stardust mission aimed to further our knowledge of interstellar dust by capturing contemporary interstellar dust grains streaming through our solar system and returning them to Earth for further analyses. The Stardust Interstellar Dust Collector was exposed to the interstellar dust stream for a total of 195 days prior to its return in 2006 (Tsou et al. 2003). The collector was largely composed of aerogel tiles (1039 cm^2), which were designed to capture hypervelocity particles with minimal damage as compared with capture in other media. The Stardust Interstellar Preliminary Examination (ISPE) was tasked with the mission of answering first-order questions regarding the interstellar collection. This included the identification, extraction, and initial analyses of tracks and residual particles that were considered candidates for interstellar dust (Westphal et al. 2014b). Because of the anticipated scarcity of captured particles, all analyses were required to be nondestructive and have the sensitivity and spatial resolution to detect the extremely small particles (typically <1 μm). These requirements limited the types of analytical methods that could be performed, and as a consequence, the ISPE analyses rely heavily on synchrotron microprobe techniques, including X-ray fluorescence (XRF), X-ray diffraction (XRD), scanning transmission X-ray

microscopy (STXM), and Fourier transform infrared (FTIR) spectromicroscopy. This paper is one of several companion papers in this issue describing the methods and analyses of the ISPE (Brenker et al. 2014; Butterworth et al. 2014; Flynn et al. 2014; Frank et al. 2013; Gainsforth et al. 2014; Postberg et al. 2014; Simionovici et al. 2014; Sterken et al. 2014; Stroud et al. 2014; Westphal et al. 2014).

Because of large uncertainties regarding the survivability of organics during hypervelocity capture in aerogel, the focus of the Stardust mission was on the refractory mineral components of cometary and interstellar dust. Nevertheless, it is now clear that some organic material in the cometary collection survived capture in aerogel (Keller et al. 2006; Sandford et al. 2006; Cody et al. 2008; Rotundi et al. 2008; Bajt et al. 2009; Elsila et al. 2009; Clemett et al. 2010; De Gregorio et al. 2010). Motivated by this, and by the scientific importance of the refractory organic component of interstellar material (Pendleton and Allamandola 2002), we participated in an effort to screen interstellar candidate particles for the presence of organic materials with FTIR spectromicroscopy.

Here, we present results from FTIR measurements that address terrestrial organic contamination in the aerogel capture media. One of the largest concerns with regard to organic contamination of the returned interstellar dust particles is the presence of carbon in the original aerogel collector tiles. This carbon is a direct result of the manufacturing process and is primarily in the form of aliphatic $–CH_3$ and $–CH_2–$ groups that are covalently bonded to the aerogel network (Tsou et al. 2003). Although the Stardust cells were heated to 300 °C for several hours to remove volatiles and minimize this organic contamination, it could not be removed completely. As a result, considerable effort was devoted to address the state, abundance, and distribution of the carbon in the original Stardust tiles. Sandford et al. (2010) present a detailed assessment of this intrinsic carbon as well as other potential sources of organic contaminants during flight and recovery that could have affected the samples captured in the cometary collector. These contaminants are also relevant to the interstellar collector and could complicate the analysis and interpretation of any organics associated with interstellar dust, particularly because signals from these particles are expected to be near or below the FTIR detection threshold.

Synchrotron FTIR spectromicroscopy is well-suited for these contamination measurements because of its high sensitivity to organics and its diffraction-limited spot size (approximately 3 μm at C–H stretching frequencies). Equally as important is the fact that infrared radiation is nonionizing and the peak and average powers on the sample are low, which make synchrotron FTIR spectromicroscopy truly noninvasive and nondestructive. The only risk of sample damage, therefore, is sample handling. Consequently, most of the interstellar candidates underwent FTIR screening prior to any other analyses. In contrast, the ionizing radiation of X-ray microprobes has the potential to damage samples, particularly under high fluence. The knowledge gained from the trace elemental analytical capabilities of these microprobes was determined to be worth the risk. Efforts were made to minimize risks to the samples by administratively controlling dose limits; however, as shown below, synchrotron FTIR measurements before and after X-ray exposure indicate that the dose limit controls did not prevent the deposition of detectable organics.

EXPERIMENTAL

Sample Preparation

Interstellar candidates were extracted from the interstellar collector in so-called picokeystones (Westphal et al. 2004; Frank et al. 2013). These wedge-shaped volumes of aerogel were machined from the aerogel collector tiles using glass needles controlled by automated micromanipulators. The candidates were located in thin (50–70 μm) sections of the picokeystones, allowing all synchrotron-based analytical techniques to be applied without removing the particle(s) from the surrounding aerogel. The picokeystones are extracted on barbed polysilicon forks, then carefully sandwiched between two 50–70 nm-thick Si_3N_4 windows (Frank et al. 2013). This mounting technique simultaneously protects the samples from contamination, reduces risk of loss by physically trapping the samples, and allows for all synchrotron-based analyses, except tomography, which has a reduced resolution due to limitations in the angular scan range.

FTIR Measurements

Infrared transmission spectra were acquired with a synchrotron-based FTIR microscope on Beamline 1.4.3 at the Advanced Light Source (ALS), Lawrence Berkeley National Laboratory (LBNL) or at Beamline U2B at the National Synchrotron Light Source (NSLS), Brookhaven National Laboratory (BNL). At both beamlines, the synchrotron source produces a diffraction-limited spot size, which is approximately 3 μm in the region of the C–H stretching frequencies (approximately 3000 cm^{-1}). Spectra were typically averaged from 16 to 4000 times, depending on the sample, and collected in the 650–4000 cm^{-1} range with 4 cm^{-1} resolution using a KBr beamsplitter and a

mercury cadmium telluride (MCT-A) detector. Silicon nitride has an absorption feature at approximately 830 cm^{-1}, but is otherwise transparent to infrared radiation. The windows were thin enough, however, to allow >30% transmission of infrared light at the absorption maximum. Thus, entire spectra in the midinfrared region could be acquired with only a minimal reduction in signal to noise around the 830 cm^{-1} absorption feature.

Spectra were normalized to a background obtained on a blank area (no aerogel) through the Si_3N_4 windows and baseline-corrected with a polynomial fit. The ratio of $–CH_2–$ to $–CH_3$ was calculated by measuring the area of the corresponding peaks at the FWHM endpoints. Because we highlight only the relative changes of these features and not the absolute number of functional groups, no attempt was made to correct for the different oscillator strengths of $–CH_2–$ and $–CH_3$ (Sandford et al. 1991; Bajt et al. 2009).

RESULTS AND DISCUSSION

A total of 27 keystones were analyzed (see Table 1): 22 keystones were considered to be interstellar candidates at some level and 5 keystones were blanks (i.e., sections of aerogel that did not contain obvious particle tracks, but still have a space-exposed surface).

Organic Contamination in Aerogel

To assess the chemical nature and distribution of indigenous carbon in the Stardust interstellar collector, numerous infrared transmission measurements were made from both Stardust flight and archival samples of unflown tiles from the same production batches. The infrared spectra of these keystones are dominated by the Si-O stretching absorption feature around 1100 cm^{-1} that is characteristic of amorphous silicates. This feature precludes any reliable measurement of silicates in interstellar dust collected in silica aerogel by FTIR spectroscopy. The carbon originally in the aerogel can be detected in the 3000–2800 cm^{-1} range, which is characteristic of the C–H stretching frequencies of aliphatic $–CH_3$ and $–CH_2–$ groups. Additional absorption features are seen near 3700 cm^{-1} ("structural O-H"), 3600–3200 cm^{-1} (adsorbed H_2O), 1700 cm^{-1} (C=O stretching), and 1640 cm^{-1} (water or other heteroatom group) (Sandford et al. 2006, 2010; Rotundi et al. 2008; Bajt et al. 2009).

As shown in Fig. 1, the spectra from different keystones vary considerably. Indeed, based on the spectral features observed in the aerogel, there appear to be at least five different classes of contamination present. The first class (bottom four rows of Fig. 1),

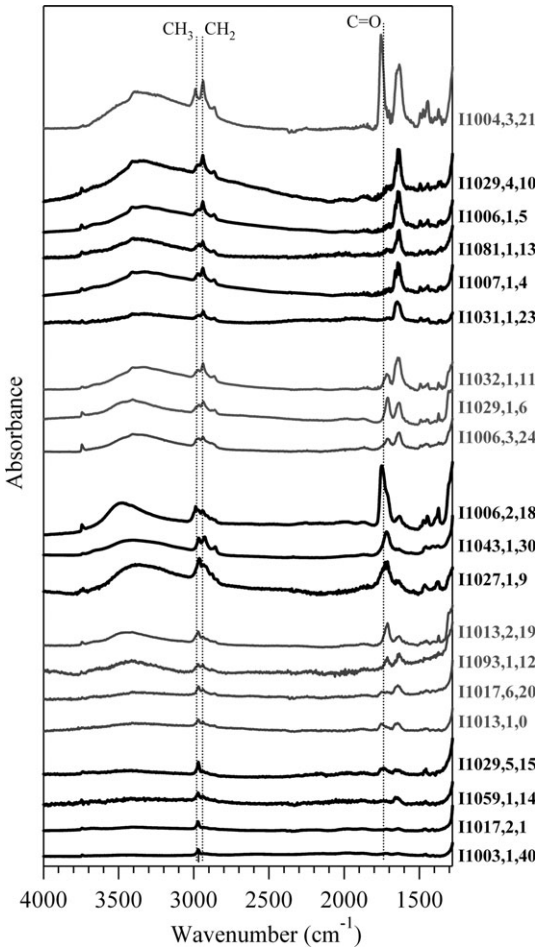

Fig. 1. Fourier transform infrared absorbance spectra of keystones extracted from the Stardust interstellar tray. All spectra were measured far from a track or terminal particle and should represent native aerogel. The spectra are grouped to highlight the different contaminant backgrounds observed in the aerogel.

represented by Tracks I1017,2,1 and I1059,1,14, I1029,5,15, and I1003,1,40 is consistent with "clean" aerogel, in which the only source of organic contaminant appears to be $Si-CH_3$ groups at approximately 2973 cm^{-1}. As mentioned previously, these $Si-CH_3$ groups are known to be the primary form of carbon in the original aerogel collector tiles, and are a direct result of the aerogel manufacturing process. The other classes represent increasing levels of contamination from other sources, including features at 1720 and 1750 cm^{-1}, which can be attributed to carbonyl groups (C=O), and at approximately 1640 cm^{-1}, which is likely adsorbed water, but could be attributed to other heteroatom groups. The biggest complication from an organic analysis perspective, however, is the increased strength of the feature at approximately 2940 cm^{-1}, which corresponds to aliphatic $–CH_2–$ groups. Unlike aerogel from the

Table 1. Interstellar keystones measured with Fourier transform infrared (FTIR) during Stardust Interstellar Preliminary Examination.

Track no.	Track description	Order of techniques	FTIR notes
I1007,4,0	Blank	XRF[a], FTIR	No signatures of XRF beam damage
I1013,1,0	Blank	FTIR, XRF[a], FTIR	Dramatic changes in aerogel after XRF measurements
I1017,1,0	Blank	XRF[a], FTIR	No signatures of XRF beam damage
I1017,4,0	Blank	FTIR, FTIR	Contaminated with cyanoacrylate after mounting in silicon nitride window
I1017,5,0	Blank	FTIR	Heat sealing caused more CH_2 contamination than Ziploc bag
I1017,2,1	Low-azimuth	XRF[a], FTIR, STXM[b], FTIR	Organic signatures associated with track, but are likely contaminants from XRF measurements
I1007,1,4	Low-azimuth	FTIR, STXM, FTIR, FTIR	No distinct organic signatures associated with track
I1006, 1,5	Low-azimuth	FTIR, XRF[c], FTIR, STXM	Dramatic changes around track after XRF measurements
I1029,1,6	9 o'clock	STXM, FTIR	No distinct organic signatures associated with track
I1027,1,9	Crater	XRF[c], FTIR, XRF[c], FTIR	No distinct organic signatures associated with track
I1029,4,10	9 o'clock	STXM, FTIR	No distinct organic signatures associated with track
I1032,1,11	Crater	STXM, FTIR	No distinct organic signatures associated with track
I1093,1,12	Crater	FTIR, XRF[c]	No distinct organic signatures associated with track
I1081,1,13	Inclusion	FTIR, XRF[c]	No distinct organic signatures associated with track
I1059,1,14	Crater	FTIR, XRF[c]	Dramatic changes around track after XRF measurements
I1029,5,15	Crater	FTIR, XRF[c], FTIR, FTIR	Dramatic changes around track after XRF measurements
I1001,1,16	Crater	XRF[d], FTIR[e]	No distinct organic signatures associated with track
I1001,2,17	Crater	XRF[d], FTIR[e]	No distinct organic signatures associated with track
I1006,2,18	Crater	STXM, FTIR	No distinct organic signatures associated with track
I1013,2,19	Crater	STXM, FTIR, FTIR, STXM, FTIR	No distinct organic signatures associated with track
I1017,6,20	Crater	FTIR, XRF[a], FTIR, STXM, FTIR	Dramatic changes around track after XRF measurements
I1004,3,21	Crater	FTIR, XRF[a], FTIR, STXM, FTIR	Contaminated with cyanoacrylate. Increased CH_3 content on picokeystone. No significant change after X-ray analyses
I1031,1,23	Crater	STXM, FTIR	No distinct organic signatures associated with track
I1006,3,24	Crater	STXM, FTIR	No distinct organic signatures associated with track
I1043,1,30	Midnight, interstellar candidate	XRF-XRD[a], STXM, XRF-XRD[c], STXM, FTIR	Organic signatures associated with track, but are likely contaminants from XRF measurements
I1092,1,37	Midnight, SRC lid	XRF[a], FTIR[e], STXM	Organic signatures associated with terminal particle
I1003,1,40	Bulbous, interstellar candidate	FTIR, STXM	No distinct organic signatures associated with track

[a]ESRF ID13.
[b]All STXM measurements at ALS 11.0.2.
[c]ESRF ID22.
[d]APS 2-ID-D.
[e]NSLS U2A, all other FTIR measurements at ALS BL 1.4.3.

cometary collector (Bajt et al. 2009; Sandford et al. 2010) where the $-CH_3$ peak is typically larger, infrared spectra of aerogel from the interstellar collector often have $-CH_2-$ peaks that are two to three times larger than the $-CH_3$ peaks, indicating larger chain lengths and more complex organic contamination.

The distribution of contaminants was measured by sampling the entire keystone using a step size of approximately 50 μm. These maps reveal few spectroscopic changes across the keystone that cannot be attributed to changes in thickness, indicating that any contamination was relatively uniform across the keystone. Thus, high resolution maps of the tracks and/or terminal particles embedded in the picokeystone could potentially reveal any organics associated with the particle. The increased $-CH_2-$ concentration in many of the keystones significantly complicates the search for organics, however, by reducing the sensitivity of the infrared measurement. The point-to-point variations in the IR spectra of the organic contamination make the precise determination of any interstellar dust organics difficult, particularly because the signal from an interstellar dust particle is expected to be exceedingly small.

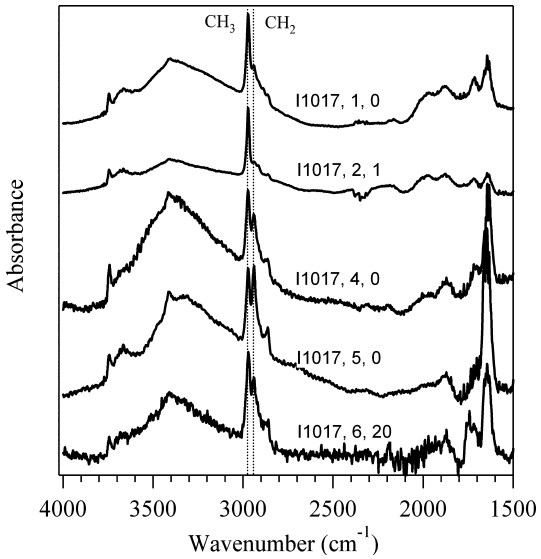

Fig. 2. Fourier transform infrared absorbance spectra of keystones extracted from cell I1017 of the Stardust interstellar tray. The variety of background contamination indicates that the organic residue from aerogel synthesis is not the only source of contamination.

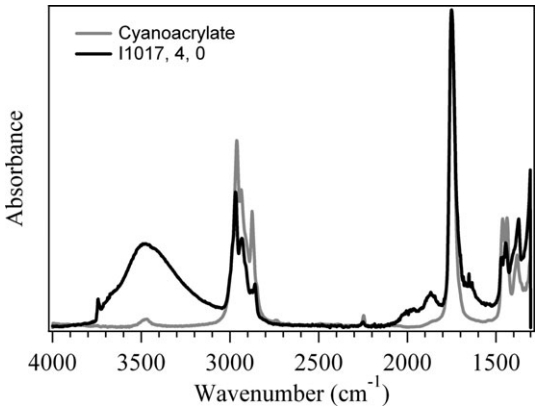

Fig. 3. Fourier transform infrared absorbance spectra (black) of I1017,4,0,0 after placement in a Si_3N_4 window sandwich and reference spectra (gray) of cyanoacrylate (HR Hummel Polymer and Additives library, Thermo-Fisher Scientific).

The source of the variation in contaminant levels from different keystones remains unknown, despite efforts to standardize extraction methods and reduce possible sources of contamination. There is no apparent correlation with extraction date, aerogel batch, or location on the Stardust collector. Indeed, as Fig. 2 indicates, contaminant levels vary considerably, even from keystones extracted from the same tile. Measurements of the physical properties of the aerogel cells indicate that the cells had quite different degrees of organic contamination immediately after synthesis and assembly (prior to flight). For example, some cells are hydrophobic, and some are hydrophilic, and some largely hydrophobic cells have hydrophilic rims, while some largely hydrophilic cells have hydrophobic cells. One possible source of this variation is the differential application of a silicone compound (Synlube 1000) that was used as a release agent to coat the aerogel mold surfaces to aid removal of the aerogel blocks**.** Although NMR measurements of aerogel samples do not show evidence of the Synlube 1000 when compared with a reference sample (Sandford et al. 2010), it is possible that the concentration of Synlube 1000 in the aerogel is below the detection limit of the NMR measurements.

The homogenous distribution of contaminants within a keystone and the lack of correlation with sample batch or location on the Stardust collector suggest that the contamination might be introduced during or after extraction. The spectra from I1017,4,0 and I1017,5,0 add additional evidence to this hypothesis. The blank keystones I1017,4,0 and I1017,5,0 were extracted sequentially, fork-mounted, and placed in standard glass bell jars for shipping on the same day. The jar for keystone I1017,5,0 was placed in a heat-sealed plastic bag to prevent external contamination during shipping, whereas the jar for keystone I1017,4,0 was wrapped in foil and placed in a Ziploc bag. As shown in Fig. 2, the contamination level of the $–CH_2–$ feature at approximately 2940 cm^{-1} for I1017,5,0 is almost double that of I1017,4,0, which might suggest that the rapid heating of the plastic bag in I1017,5,0 released volatile organics that were readily absorbed by the aerogel. The keystone I1017,4,0 is by no means free of contamination, however, and the increased $–CH_2–$ content in I1017,5,0 may have been a coincidence. Regardless, the heat-sealing technique has been discontinued and other efforts have been made to reduce the amount of plastics used for shipping and storage.

Figure 3 shows that sealing the Si_3N_4 windows with cyanoacrylate, another common procedure (Frank et al. 2013), has the potential to introduce contamination in the keystone. Spectra were measured on keystone I1017,4,0 after placement in a Si_3N_4 window "sandwich." The peaks at approximately 1751 cm^{-1} (C=O stretch) and approximately 2248 cm^{-1} (C≡N) agree quite well with reference spectra of cyanoacrylate (HR Hummel Polymer and Additives library, Thermo-Fisher Scientific). The fact that this keystone did not show these features when it was fork-mounted (see Fig. 2) provides unambiguous evidence that this contamination was from mounting procedures. These features are not, however, prevalent in most of the measured keystones. Indeed, only one other keystone, I1004,3,21, has observable peaks that are characteristic of cyanoacrylate. The window mounting process has

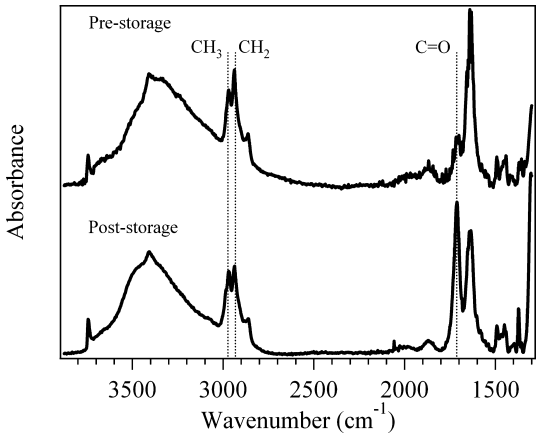

Fig. 4. Fourier transform infrared absorbance spectra in the C–H stretching region of keystone I1007,1,4 before and after 9 months of storage. The spectra have been offset for clarity.

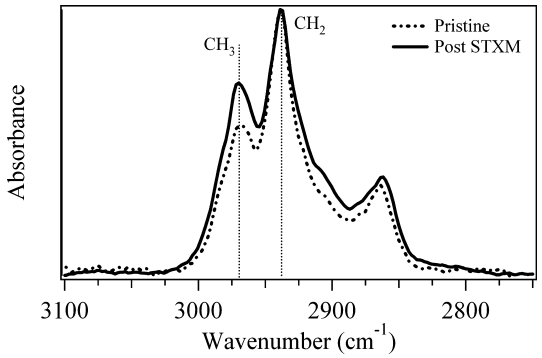

Fig. 5. Fourier transform infrared absorbance spectra in the C–H stretching region of keystone I1007,1,4 before (dotted) and after (solid) scanning transmission X-ray microscopy analysis at the Advanced Light Source. The spectra have been normalized to the CH_2 peak at 2940 cm^{-1} for easier comparison.

been improved to reduce the amount of cyanoacrylate used in the sealing process (Frank et al. 2013).

Figure 4 presents additional evidence that the aerogel keystones are being contaminated during storage. FTIR measurements of I1007,1,4 show dramatically different spectra before and after 9 months of storage in a nitrogen-filled purge. In particular, there is a large increase in the C=O peak at 1712 cm^{-1}, subtle changes in the–OH band, and a change in the $–CH_2–$/$–CH_3$ ratio. These changes appear to be homogeneously distributed throughout the keystone, as observed for other keystones. It is unclear if the change in the FTIR spectra was a result of a one-time incident, perhaps during sample transfer, or if the changes were gradual over the course of the storage period. Nevertheless, samples are now stored in an organics-free nitrogen purge.

Beam Damage from X-Ray Microprobes

While synchrotron infrared measurements have the potential to provide a measure of the organic content within samples, they cannot compete with X-ray microprobes in terms of elemental and mineralogical analysis, which is critical for identifying samples of terrestrial origin. Consequently, picokeystones from the interstellar collector tray were sent to several synchrotrons for XRF, XRD, and STXM analyses. Although these techniques are considered minimally invasive, X-rays are a form of ionizing radiation and have the potential to cause beam damage under conditions of high fluence and small focal spots. To monitor the effects of these X-ray microprobes, infrared spectra were taken before and after X-ray analyses.

Figure 5 shows infrared spectra in the C–H stretching region of I1007,1,4 before and after STXM analysis at the ALS Beamline 11.0.2. The spectra have been normalized to the $–CH_2–$ peak at 2940 cm^{-1}. There is a small change in the $–CH_2–$ (2940 cm^{-1})/$–CH_3$ (2970 cm^{-1}) ratio that is statistically significant compared with the fluctuations within the aerogel. The change in this ratio, however, appears to be distributed throughout the picokeystone and not only around the terminal particle, as would be expected if this change arises from STXM analysis. There was approximately 1 month between the initial FTIR analysis on the pristine sample and the FTIR analysis after the STXM measurements. As noted above, this keystone showed dramatic changes in its spectra after 9 months of storage (post-STXM), so it is likely that the differences observed before and after STXM measurements are the result of storage contamination and not STXM-induced. Examination of three other keystones (I1004,3,21; I1017,2,1; and I1017,6,20) before and after STXM analysis showed essentially no changes in the C–H stretching region of the spectra. These three keystones, however, were analyzed by XRF prior to STXM, so it is possible that any damage that could have been done to the aerogel by X-rays already occurred during the XRF analysis. Nevertheless, there is no strong evidence that the STXM measurements cause any damage to the terminal particles or surrounding aerogel for these samples.

In contrast, hard XRF and/or XRD measurements appear to dramatically alter the organic content in the aerogel. Figure 6 shows infrared spectra in the C–H stretching region of I1017,6,20 before and after XRF/XRD analysis at the European Synchrotron Radiation Facility beamline ID13 (Brenker et al. 2014; Gainsforth et al. 2014). The $–CH_2–$/$–CH_3$ ratio is altered, and a new $–CH_3$ feature appears at approximately 2990 cm^{-1}. Six of the nine keystones measured after XRF/XRD

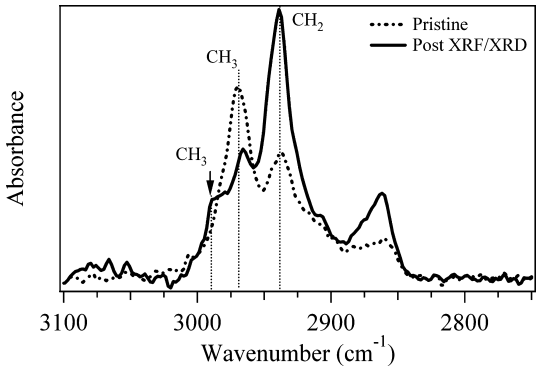

Fig. 6. Fourier transform infrared absorbance spectra in the C–H stretching region of keystone I1017,6,20 before (dotted) and after (solid) X-ray fluorescence analysis at European synchrotron radiation facility ID13. The arrow indicates the shoulder at 2988 cm^{-1} that is characteristic of X-ray beam damage.

analysis at ESRF ID13 or ID22 show this characteristic feature. Moreover, as shown in Fig. 7, these changes are only seen around the track and/or terminal particle, indicating that the approximately 2990 cm^{-1} feature is beam-induced and not from other sources of external contamination that could occur during shipping or storage.

Dosing limits for the X-ray analyses were established by approximating the integrated fluence of cosmic X-rays an interstellar particle would be expected to receive during its average residence time in our solar system. For the ESRF ID22 beam characteristics, this yields a fluence of about 3×10^{19} photons cm^{-2}, which was deemed to be the astronomical limit (AL) (Simionovici et al. 2011, 2014). Although all synchrotron measurements were intended to be below the AL, beam monitoring errors led in some cases to irradiation fluences greater than 50 times the AL. Additional evidence from STXM measurements indicates that the XRF measurements contributed to radial smearing and the loss of mass of some terminal particles (Butterworth et al. 2014; Simionovici et al. 2014).

Interstellar Candidates

Many of the tracks discovered in the interstellar collector are consistent in their trajectories with an origin as secondary ejecta from the spacecraft, but 24 tracks have been identified with trajectories that are consistent with an origin either in the interstellar dust stream or as ejecta from impacts on the lid of the sample return capsule. Twleve of these so-called "midnight" tracks have been examined by ISPE thus far (Frank et al. 2013), and three are inconsistent in their origin with secondary ejecta based on subsequent X-ray microprobe elemental analysis: Track I1043,1,30 (Track

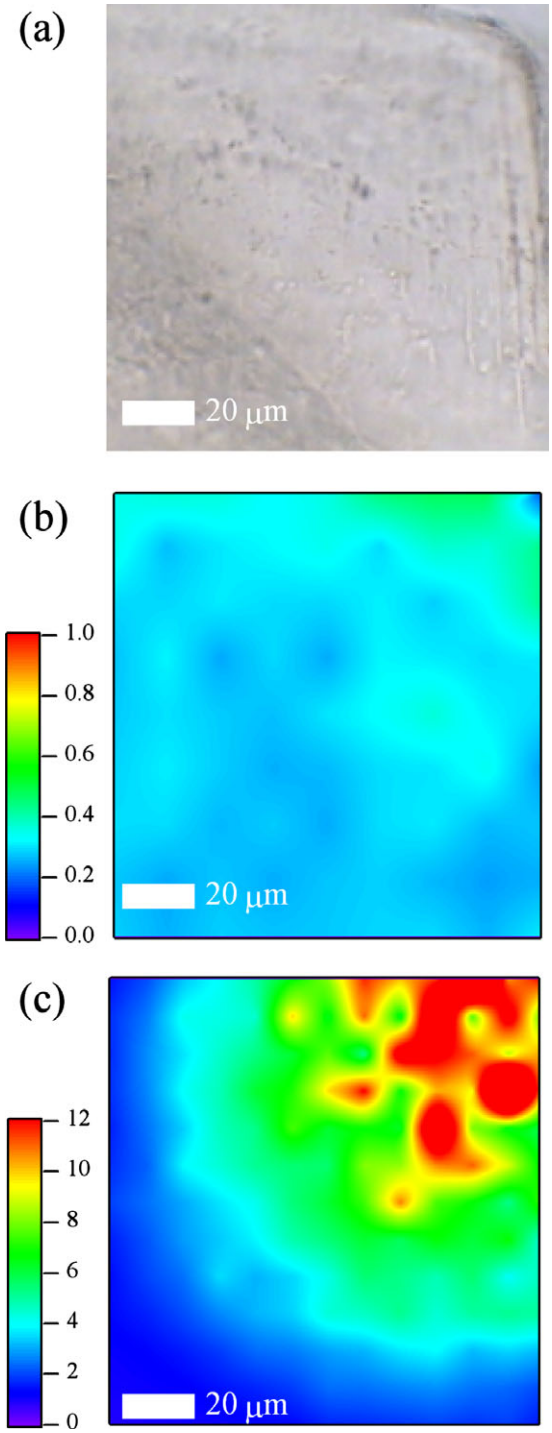

Fig. 7. a) Optical image of I1017,6,20 keystone. The space-exposed surface is at the top of the image and the diagonal line in the lower left corner is the step between the normal keystone and the picokeystone. b) Image map corresponding to the $–CH_2–/–CH_3$ area ratio measured on the keystone prior to any synchrotron X-ray analysis. c) Image map corresponding to the $–CH_2–/–CH_3$ area ratio measured on the keystone after X-ray fluorescence analysis on European Synchrotron Radiation Facility ID13. Note change in color scale.

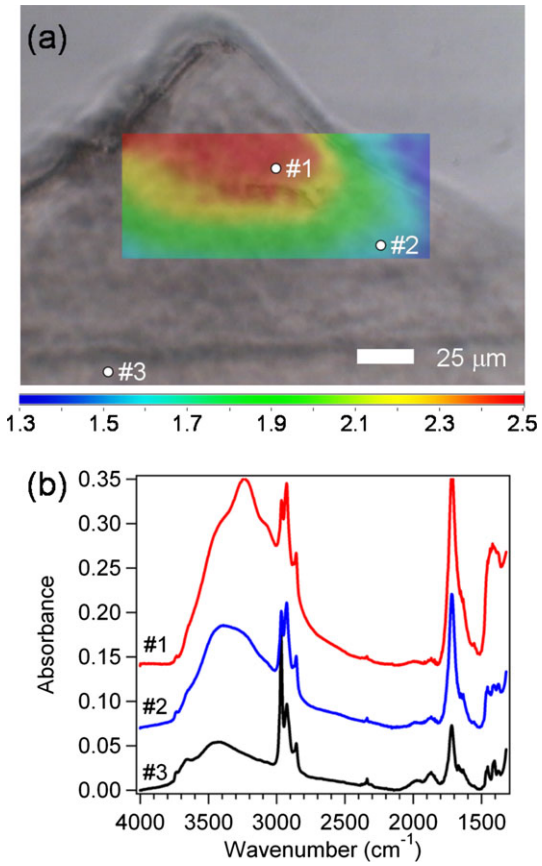

Fig. 8. a) Fourier transform infrared image map of I1043,1,30,0,0, corresponding to the $–CH_2–/–CH_3$ area ratio, superimposed on an optical image of the keystone. b) FTIR spectra of several points in the keystone, as indicated in (a).

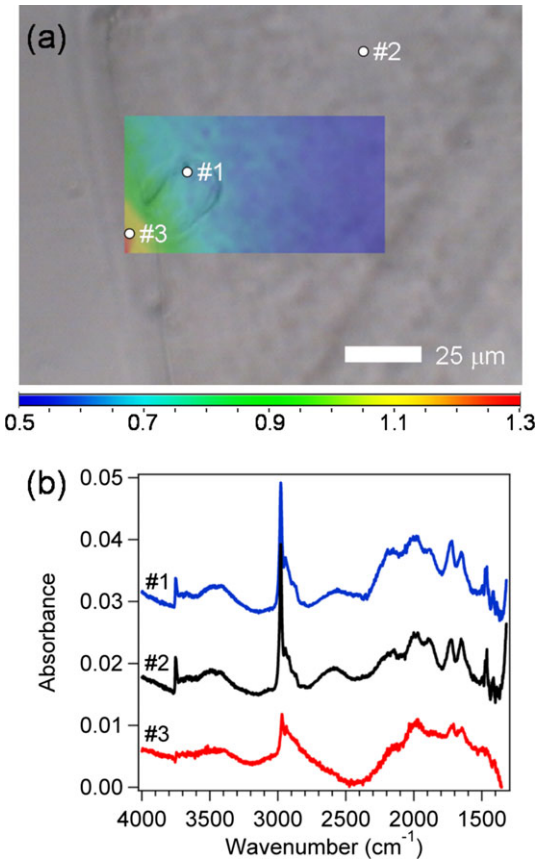

Fig. 9. a) Fourier transform infrared image map of I1003,1,40,0,0, corresponding to the $–CH_2–/–CH_3$ area ratio, superimposed on an optical image of the keystone. b) FTIR spectra of several points in the keystone, as indicated in (a).

30, "Orion/Sirius"), Track I1047,1,34 (Track 34, "Hylabrook"), and Track I1003,1,40 (Track 40, "Sorok") (Butterworth et al. 2014).

Track 30 contains two terminal particles, "Orion" and "Sirius," that were believed to be weakly bound at the time of capture. Figure 8 shows FTIR image maps and spectra taken in and around Track 30. As shown in Fig. 8a, there is a clear change in the $–CH_2–/–CH_3$ area ratio around the terminal particles. Unfortunately, this keystone was measured with STXM and XRF prior to any FTIR analyses. As shown above, hard X-ray XRF measurements have the propensity to damage the aerogel and increase the level of CH_2 contamination. This keystone has obvious optical damage, and so it is highly likely that the organic signatures found around the terminal particles are X-ray induced beam damage and not native to the particles.

Track 34 (I1047,1,34) contains one terminal particle, "Hylabrook." It has been examined via XRF and STXM, but it was never allocated for FTIR analysis. It is likely that the XRF measurements contaminated the keystone with organics, so any FTIR analyses at this point would provide ambiguous results.

Track 40 (I1003,1,40) is a high-velocity impact with a capture speed estimated to be greater than 15 km s^{-1} (Postberg et al. 2014). Unlike Tracks 30 and 34, there are no obvious terminal particles associated with the track. This keystone was examined via FTIR prior to any X-ray analyses, and as a consequence does not suffer any ambiguities about possible beam damage. Furthermore, spectra taken on the picokeystone and main keystone indicate that there is minimal organic contamination within the keystone, making it an ideal candidate for organic analyses. Figure 9 shows FTIR image maps and spectra taken in and around Track 40. Although there is a small change in the $–CH_2–/–CH_3$ ratio (see Fig. 9a) at the space-exposed surface of the keystone, there do not appear to be any organics associated with the track deeper in the keystone. The change in the $–CH_2–/–CH_3$ ratio at the aerogel surface has been observed in other keystones without tracks, so it is unlikely that this feature is related to the impact or track.

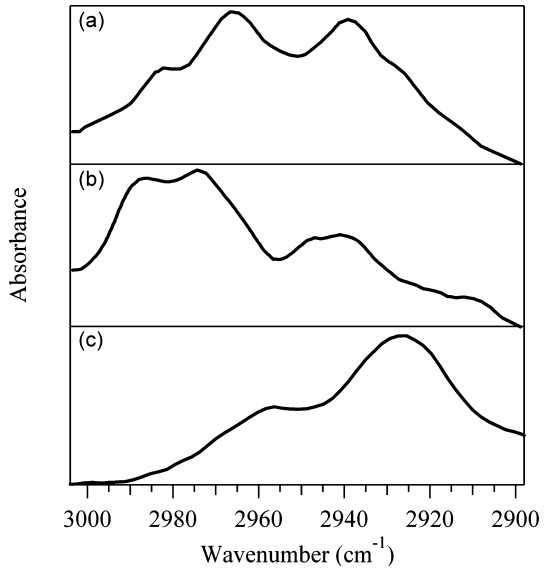

Fig. 10. Infrared transmittance spectra of the terminal particle of a) track 37, "Merlin," and of the b) aerogel approximately 40 μm past the terminal particle along the extension of the normal to the aerogel surface and passing through the terminal particle. Both spectra were taken under similar conditions using a 5 μm × 5 μm aperture. The third spectrum (c) is a reflectance measurement of a sample of the SRC deck.

As discussed above, the sensitivity of the FTIR measurements is compromised by the presence of terrestrial organic contamination. This degraded sensitivity, plus the small size of the samples, and the high-velocity collection method, certainly make the search for organics in the interstellar candidates a challenging process. The keystone I1092,1,37 (Track 37, "Merlin"), however, offers a glimmer of hope that organics are detectable if present in sufficient quantities. The shape and trajectory of Track 37, a 62 mm long "midnight" track with an optically visible terminal particle ("Merlin"), indicate that the collection velocity was similar to that of the interstellar candidates, but STXM measurements have identified ("Merlin") as a secondary impact because its composition resembles the SRC deck (Butterworth et al. 2014). FTIR spectra (Fig. 10) of the terminal particle, for which STXM measurements indicate an approximately 0.5 × 1.0 μm Al hot spot having about equal amounts of Al and C (Butterworth et al. 2014), show organic features that are distinct from the aerogel background contamination. Track 37 was analyzed via XRF (Brenker et al. 2014) prior to FTIR analyses, however, so there is a possibility of contamination from X-rays. Those measurements, however, involved only a fast survey scan, which failed to locate the terminal particle, consequently resulting in minimal X-ray dosing. Because the distinct organic features were only found at the location of the terminal particle and not in the surrounding aerogel, it is unlikely that X-ray damage is the source of the organic features.

Fourier transform infrared reflection measurements taken on a sample of the SRC deck also reveal organic compounds on the surface. However, the C–H stretch region is dramatically different than the spectra measured from "Merlin" in Track 37 (see Fig. 10). This could indicate that the original organics were modified during the high-velocity capture event, which certainly raises questions about the relevance of any organics associated with Stardust interstellar particles that might be found in the future. Alternatively, the surface of the SRC deck could have easily been contaminated with other terrestrial organics during its transfer, storage, and nearly 5 yr display at the Smithsonian Air and Space museum before the sample was extracted. Thus, it is entirely possible that the recent measurements of organics on the SRC deck sample have no relevance to the organics that were present during the interstellar collection period. Regardless, the detection of organics in "Merlin" increases the confidence that FTIR has the sensitivity to detect organics from particles within the "dirty" aerogel, and thereby make the search worthwhile.

CONCLUSIONS

An FTIR survey of 27 picokeystones extracted from the Stardust Interstellar Dust Collector provides evidence that terrestrial organic contamination of these rare samples occurred after extraction during sample storage and hard X-ray XRF measurements. The absorption of volatile organics appears to be the primary source of contamination during storage and/or sample transfer, as indicated by the homogenous distribution of contaminants throughout the picokeystones; however, contamination during flight, re-entry, and/or recovery cannot be ruled out. Although this contamination reduces the sensitivity of the FTIR measurement by increasing background organic content, organics associated with interstellar dust can still be distinguished from the organic contamination by comparing spectra obtained on the track and/or terminal particle with spectra obtained off the track/particle. Nevertheless, efforts have been made to reduce the exposure of the picokeystones to plastics and other sources of volatile organics.

The damage induced by the hard X-ray XRF measurements is more problematic than sample storage contamination. Because damage occurs only where the X-ray beam is scanned, which is primarily around the track and terminal particles, there is no convenient method to differentiate organics associated with the

interstellar dust particle from the organics associated with X-ray beam damage. One solution is to perform the FTIR analyses of the picokeystones prior to any X-ray analysis. This procedure has been adopted and is logical because the nonionizing nature of infrared radiation means that the only risk of sample damage is sample handling. One disadvantage of this procedure, however, is that it precludes other organic analyses from being performed at a later time because there is no confidence that the measurements after X-ray exposure will reveal organics that are actually indigenous to interstellar dust.

The ISPE has recently identified three Level 2 impacts that have a trajectory consistent with interstellar origin and a composition inconsistent with spacecraft materials (Westphal et al. 2014b). Of the three tracks, two were examined via X-ray techniques prior to FTIR, making the interpretation of the signals difficult. The third track, Track 40, was examined via FTIR prior to other analyses, and we can confidently state that any organics, if present, are below the detection limit. This particular track is consistent with a high-speed capture and does not contain evidence of any terminal particles. Thus, it is conceivable that any organics that were originally present in the original particle were vaporized by the collection event.

Astronomical infrared observations suggest that aliphatic –CH groups in interstellar dust grains are widespread and may be an important reservoir of prebiotic organic carbon. Although it has not been possible to identify the specific hydrocarbon materials associated with the strong emission feature near 2940 cm^{-1} (3.4 μm), comparisons with laboratory interstellar analogs indicate that this feature primarily originates from short, saturated aliphatic chains. Longer alkane chains $H_3C–(CH_2)_n$ with n much larger than four or five do not appear to be major constituents in interstellar dust (Sandford et al. 1991; Pendleton and Allamandola 2002). It is unclear as to whether any of this material would survive the high-velocity capture, but if organics were found to be associated with some of the interstellar candidates, it would help answer many questions regarding the carrier of these organic features. Despite the challenges, synchrotron FTIR microscopy continues to be a good technique for the detection of organic signatures in interstellar candidates because of its high sensitivity, low risk, and nondestructive nature.

Acknowledgments—The ISPE consortium gratefully acknowledges the NASA Discovery Program for Stardust, the fourth NASA Discovery mission. GJF was supported by a NASA Laboratory Analysis of Returned Samples research grant NNX11AE15G. AJW, ALB, ZG, RL, DZ, WM, and JVK were supported by NASA grant NNX09AC36G. RMS, HCG, and NDB were supported by NASA grant NNH11AQ61I. The ALS is supported by the Director, Office of Science, Office of Basic Energy Sciences, of the U.S. Department of Energy under Contract No. DE-AC02-05CH11231. Use of the NSLS, BNL, was supported by the U.S. Department of Energy, Office of Science, Office of Basic Energy Sciences, under Contract No. DE-AC02-98CH10886.

Editorial Handling—Dr. John Bradley

REFERENCES

Bajt S., Sandford S. A., Flynn G. J., Matrajt G., Snead C. J., Westphal A. J., and Bradley J. P. 2009. Infrared spectroscopy of Wild 2 particle hypervelocity tracks in Stardust aerogel: Evidence for the presence of volatile organics in cometary dust. *Meteoritics & Planetary Science* 44:471–484.

Bernstein R. A., Freedman W. L., and Madore B. F. 2002. The first detections of the extragalactic background light at 3000, 5500, and 8000 angstrom III. Cosmological implications. *The Astrophysical Journal* 571:107–128.

Brenker F. E., Schoonjans T., Silversmit G., Vekemans B., Vincze L., Westphal A. J., Allen C., Anderson D., Ansari A., Bajt S., Bastien R. S., Bassim N., Bechtel H. A., Borg J., Bridges J., Brownlee D. E., Burchell M., Burghammer M., Butterworth A. L., Changela H., Cloetens P., Davis A. M., Doll R., Floss C., Flynn G., Fougeray P., Frank D. R., Gainsforth Z., Grün E., Heck P. R., Hillier J. K., Hoppe P., Hudson B., Huth J., Hvide B., Kearsley A., King A. J., Lai B., Leitner J., Lemelle L., Leroux H., Leonard A., Lettieri R., Marchant W., Nittler L. R., Ogliore R., Ong W. J., Postberg F., Price M. C., Sandford S. A., Sans Tresseras J., Schmitz S., Simionovici A. S., Solé V. A., Srama R., Stephan T., Sterken V. J., Stodolna J., Stroud R. M., Sutton S., Trieloff M., Tsou P., Tsuchiyama A., Tyliszczak T., Korff J. V., Wordsworth N., Zevin D., Zolensky M. E., and >30,000 Stardust@home dusters. 2014. Stardust Interstellar Preliminary Examination V: XRF analyses of interstellar dust candidates at ESRF ID13. *Meteoritics & Planetary Science*, doi:10.1111/maps.12206.

Butterworth A., Westphal A. J., Tyliszczak T., Gainsforth Z., Stodolna J., Frank D. R., Allen C., Anderson D., Ansari A., Bajt S., Bastien R. S., Bassim N., Bechtel H. A., Borg J., Brenker F. E., Bridges J., Brownlee D. E., Burchell M., Burghammer M., Changela H., Cloetens P., Davis A. M., Doll R., Floss C., Flynn G., Grün E., Heck P. R., Hillier J. K., Hoppe P., Hudson B., Huth J., Hvide B., Kearsley A., King A. J., Lai B., Leitner J., Lemelle L., Leroux H., Leonard A., Lettieri R., Marchant W., Nittler L. R., Ogliore R., Ong W. J., Postberg F., Price M. C., Sandford S. A., Sans Tresseras J., Schmitz S., Schoonjans T., Silversmit G., Simionovici A. S., Solé V. A., Srama R., Stephan T., Sterken V. J., Stroud R. M., Sutton S., Trieloff M., Tsou P., Tsuchiyama A., Vekemans B., Vincze L., Korff J. V., Wordsworth N., Zevin D., Zolensky M. E., and >30,000 Stardust@home dusters. 2014. Stardust Interstellar Preliminary Examination IV:

Scanning transmission X-ray microscopy analyses of impact features in the Stardust Interstellar Dust Collector. *Meteoritics & Planetary Science*, doi:10.1111/maps.12220.

Clemett S. J., Sandford S. A., Nakamura-Messenger K., Hoerz F., and McKay D. S. 2010. Complex aromatic hydrocarbons in Stardust samples collected from comet 81P/Wild 2. *Meteoritics & Planetary Science* 45:701–722.

Cody G. D., Ade H., Alexander C. M. O'D., Araki T., Butterworth A., Fleckenstein H., Flynn G., Gilles M. K., Jacobsen C., Kilcoyne A. L. D., Messenger K., Sandford S. A., Tyliszczak T., Westphal A. J., Wirick S., and Yabuta H. 2008. Quantitative organic and light-element analysis of comet 81P/Wild 2 particles using C-, N-, and O-mu-XANES. *Meteoritics & Planetary Science* 43:353–365.

De Gregorio B. T., Stroud R. M., Nittler L. R., Alexander C. M. O'D., and Kilcoyne A. L. D. 2010. Isotopic anomalies in organic nanoglobules from comet 81P/Wild 2: Comparison to Murchison nanoglobules and isotopic anomalies induced in terrestrial organics by electron irradiation. *Geochimica et Cosmochimica Acta* 74:4454–4470.

Draine B. T. 2003. Interstellar dust grains. *Annual Review of Astronomy and Astrophysics* 41:241–289.

Elsila J. E., Glavin D. P., and Dworkin J. P. 2009. Cometary glycine detected in samples returned by Stardust. *Meteoritics & Planetary Science* 44:1323–1330.

Flynn G. S. S., Lai B., Wirick S., Allen C., Anderson D., Ansari A., Bajt S., Bastien R. S., Bassim N., Bechtel H. A., Borg J., Brenker F. E., Bridges J., Brownlee D. E., Burchell M., Burghammer M., Butterworth A. L., Changela H., Cloetens P., Davis A. M., Doll R., Floss C., Frank D. R., Gainsforth Z., Grün E., Heck P. R., Hillier J. K., Hoppe P., Hudson B., Huth J., Hvide B., Kearsley A., King A. J., Leitner J., Lemelle L., Leroux H., Leonard A., Lettieri R., Marchant W., Nittler L. R., Ogliore R., Ong W. J., Postberg F., Price M. C., Sandford S. A., Tresseras J. S., Schmitz S., Schoonjans T., Silversmit G., Simionovici A., Solé V. A., Srama R., Stephan T., Sterken V. J., Stodolna J., Stroud R. M., Trieloff M., Tsou P., Tsuchiyama A., Tyliszczak T., Vekemans B., Vincze L., Korff J. V., Westphal A. J., Wordsworth N., Zevin D., Zolensky M. E., and >30,000 Stardust@home dusters. 2014. Stardust Interstellar Preliminary Examination VII: Synchrotron X-ray fluorescence analysis of six Stardust interstellar candidates measured with the advanced photon source 2-ID-D microprobe. *Meteoritics & Planetary Science*, doi:10.1111/maps.12144.

Frank D. R., Westphal A. J., Zolensky M. E., Bastien R. K., Gainsforth Z., Allen C., Anderson D., Ansari A., Bajt S., Bassim N., Bechtel H. A., Borg J., Brenker F. E., Bridges J., Brownlee D. E., Burchell M., Burghammer M., Butterworth A. L., Changela H., Cloetens P., Davis A. M., Doll R., Floss C., Flynn G., Grün E., Heck P. R., Hillier J. K., Hoppe P., Hudson B., Huth J., Hvide B., Kearsley A., King A. J., Lai B., Leitner J., Lemelle L., Leroux H., Leonard A., Lettieri R., Marchant W., Nittler L. R., Ogliore R., Ong W. J., Postberg F., Price M. C., Sandford S. A., Tresseras J. S., Schmitz S., Schoonjans T., Silversmit G., Simionovici A. S., Solé V. A., Srama R., Stephan T., Sterken V. J., Stodolna J., Stroud R. M., Sutton S., Trieloff M., Tsou P., Tsuchiyama A., Tyliszczak T., Vekemans B., Vincze L., Korff J. V., Wordsworth N., Zevin D, and >30,000 Stardust@Home Dusters. 2013. Stardust Interstellar Preliminary Examination II: Curating the interstellar dust collector, picokeystones, and sources of impact tracks. *Meteoritics & Planetary Science*, doi:10.1111/maps.12147.

Gainsforth Z., Brenker F. E., Burghammer M., Simionovici A. S., Schmitz S., Cloetens P., Lemelle L., Sans Tresseras J., Schoonjans T., Silversmit G., Solé V. A., Vekemans B., Vincze L., Westphal A. J., Allen C., Anderson D., Ansari A., Bajt S., Bastien R. S., Bassim N., Bechtel H. A., Borg J., Bridges J., Brownlee D. E., Burchell M., Butterworth A. L., Changela H., Davis A. M., Doll R., Floss C., Flynn G., Frank D. R., Grün E., Heck P. R., Hillier J. K., Hoppe P., Hudson B., Huth J., Hvide B., Kearsley A., King A. J., Lai B., Leitner J., Leroux H., Leonard A., Lettieri R., Marchant W., Nittler L. R., Ogliore R., Ong W. J., Postberg F., Price M. C., Sandford S. A., Srama R., Stephan T., Sterken V. J., Stodolna J., Stroud R. M., Sutton S., Trieloff M., Tsou P., Tsuchiyama A., Tyliszczak T., Korff J. V., Wordsworth N., Zevin D., Zolensky M. E., and >30,000 Stardust@home dusters. 2014. Stardust Interstellar Preliminary Examination VIII: Identification of crystalline material in two interstellar candidates. *Meteoritics & Planetary Science*, doi:10.1111/maps.12148.

Henning T. 2010. Cosmic silicates. *Annual Review of Astronomy and Astrophysics* 48:21–46.

Keller L. P., Bajt S., Baratta G. A., Borg J., Bradley J. P., Brownlee D. E., Busemann H., Brucato J. R., Burchell M., Colangeli L., D'hendecourt L., Djouadi Z., Ferrini G., Flynn G., Franchi I. A., Fries M., Grady M. M., Graham G. A., Grossemy F., Kearsley A., Matrajt G., Nakamura-Messenger K., Mennella V., Nittler L., Palumbo M. E., Stadermann F. J., Tsou P., Rotundi A., Sandford S. A., Snead C., Steele A., Wooden D., and Zolensky M. 2006. Infrared spectroscopy of comet 81P/Wild 2 samples returned by Stardust. *Science* 314:1728–1731.

Pendleton Y. J., and Allamandola L. J. 2002. The organic refractory material in the diffuse interstellar medium: Mid-infrared spectroscopic constraints. *The Astrophysical Journal Supplemental Series* 138:75–98.

Postberg F., Hillier J. K., Armes S. P., Bugiel S., Butterworth A. L., Dupin D., Fielding L. A., Fujii S., Gainsforth Z., Grün E., Li Y. W., Srama R., Sterken V. J., Stodolna J., Trieloff M., Westphal A. J., Allen C., Anderson D., Ansari A., Bajt S., Bastien R. S., Bassim N., Bechtel H. A., Borg J., Brenker F. E., Bridges J., Brownlee D. E., Burchell M., Burghammer M., Changela H., Cloetens P., Davis A. M., Doll R., Floss C., Flynn G., Frank D. R., Heck P. R., Hoppe P., Hudson B., Huth J., Hvide B., Kearsley A., King A. J., Lai B., Leitner J., Lemelle L., Leroux H., Leonard A., Lettieri R., Marchant W., Nittler L. R., Ogliore R., Ong W. J., Price M. C., Sandford S. A., Tresseras J. S., Schmitz S., Schoonjans T., Silversmit G., Simionovici A., Solé V. A., Stephan T., Stroud R. M., Sutton S., Tsou P., Tsuchiyama A., Tyliszczak T., Vekemans B., Vincze L., Korff J. V., Wordsworth N., Zevin D., Zolensky M. E., and >30,000 Stardust@home dusters. 2014. Stardust Interstellar Preliminary Examination IX: High speed interstellar dust analogue capture in Stardust flight-spare aerogel. *Meteoritics & Planetary Science*, doi:10.1111/maps.12173.

Rotundi A., Baratta G. A., Borg J., Brucato J. R., Busemann H., Colangeli L., D'hendecourt L., Djouadi Z., Ferrini G., Franchi I. A., Fries M., Grossemy F., Keller L. P., Mennella V., Nakamura K., Nittler L. R., Palumbo M. E.,

Sandford S. A., Steele A., and Wopenka B. 2008. Combined micro-Raman, micro-infrared, and field emission scanning electron microscope analyses of comet 81P/Wild 2 particles collected by Stardust. *Meteoritics & Planetary Science* 43:367–397.

Sandford S. A., Allamandola L. J., Tielens A., Sellgren K., Tapia M., and Pendleton Y. 1991. The interstellar C–H stretching band near 3.4 microns—Constraints on the composition of organic material in the diffuse interstellar-medium. *The Astrophysical Journal* 371:607–620.

Sandford S. A., Aleon J., Alexander C. M. O. D., Araki T., Bajt S., Baratta G. A., Borg J., Bradley J. P., Brownlee D. E., Brucato J. R., Burchell M. J., Busemann H., Butterworth A., Clemett S. J., Cody G., Colangeli L., Cooper G., D'hendecourt L., Djouadi Z., Dworkin J. P., Ferrini G., Fleckenstein H., Flynn G. J., Franchi I. A., Fries M., Gilles M. K., Glavin D. P., Gounelle M., Grossemy F., Jacobsen C., Keller L. P., Kilcoyne A. L. D., Leitner J., Matrajt G., Meibom A., Mennella V., Mostefaoui S., Nittler L. R., Palumbo M. E., Papanastassiou D. A., Robert F., Rotundi A., Snead C. J., Spencer M. K., Stadermann F. J., Steele A., Stephan T., Tsou P., Tyliszczak T., Westphal A. J., Wirick S., Wopenka B., Yabuta H., Zare R. N., and Zolensky M. E. 2006. Organics captured from comet 81P/Wild 2 by the Stardust spacecraft. *Science* 314:1720–1724.

Sandford S. A., Bajt S., Clemett S. J., Cody G. D., Cooper G., Degregorio B. T., De Vera V., Dworkin J. P., Elsila J. E., Flynn G. J., Glavin D. P., Lanzirotti A., Limero T., Martin M. P., Snead C. J., Spencer M. K., Stephan T., Westphal A., Wirick S., Zare R. N., and Zolensky M. E. 2010. Assessment and control of organic and other contaminants associated with the Stardust sample return from comet 81P/Wild 2. *Meteoritics & Planetary Science* 45:406–433.

Simionovici A., Allen C., Bajt S., Bastien R., Bechtel H., Borg J., Brenker F. E., Bridges J. C., Brownlee D. E., Burchell M. J., Burghammer M., Butterworth A., Cloetens P., Davis A. M., Floss C., Flynn G., Frank D., Gainsforth Z., Gruen E., Heck P. R., Hillier J., Hoppe P., Howard L., Huss G. R., Huth J., Kearsley A. T., King A. J., Lai B., Leitner J., Lemelle L., Leroux H., Lettieri R., Marchant W., Nittler L., Ogliore R., Postberg F., Sandford S., Tresseras J. A. S., Schoonjans T., Schmitz S., Silversmit G., Sole V. A., Srama R., Stephan T., Stodolna J., Stroud R. M., Sutton S., Trieloff M., Tsou P., Tsuchiyama A., Tyliczs-Zak T., Vekemans B., Vincze L., Westphal A. J., Zevin D., and Zolensky M. E. 2011a. Synchrotron X-ray irradiation of Stardust interstellar candidates: From "no" to "low" damage effects. *Meteoritics & Planetary Science* 46:A213–A213.

Simionovici A. S., Allen C., Bajt S., Bastien R., Bechtel H., Borg J., Brenker F. E., Bridges J. C., Brownlee D. E., Burchell M. J., Burghammer M., Butterworth A., Cloetens P., Davis A. M., Floss C., Flynn G., Frank D., Gainsforth Z., Grun E., Heck P. R., Hillier J., Hoppe P., Howard L., Huss G. R., Huth J., Kearsley A. T., King A. J., Lai B., Leitner J., Lemelle L., Leroux H., Lettieri R., Marchant W., Nittler L., Ogliore R., Postberg F., Sandford S., Tresseras J. A. S., Schoonjans T., Schmitz S., Silversmit G., Sole V. A., Srama R., Stephan T., Stodolna J., Stroud R. M., Sutton S., Trieloff M., Tsou P., Tsuchiyama A., Tyliczs-Zak T., Vekemans B., Vincze L., Westphal A. J., Zevin D., and Zolensky M. E. 2011b. Synchrotron radiation microprobe effects on Stardust interstellar dust candidates. LPI Contribution 1608. Houston, Texas: Lunar and Planetary Institute. 2812 p. 42nd Lunar and Planetary Science Conference, held March 7–11, 2011 at The Woodlands, Texas. LPI Contribution No. 1608, p.2812.

Simionovici A. S., Lemelle L., Cloetens P., Solé V. A., Sans Tresseras J., Butterworth A. L., Westphal A. J., Gainsforth Z., Stodolna J., Allen C., Anderson D., Ansari A., Bajt S., Bassim N., Bastien R. S., Bechtel H. A., Borg J., Brenker F. E., Bridges J., Brownlee D. E., Burchell M., Burghammer M., Changela H., Davis A. M., Doll R., Floss C., Flynn G., Frank D. R., Grün E., Heck P. R., Hillier J. K., Hoppe P., Hudson B., Huth J., Hvide B., Kearsley A., King A. J., Lai B., Leitner J., Leonard A., Leroux H., Lettieri R., Marchant W., Nittler L. R., Ogliore R., Ong W. J., Postberg F., Price M. C., Sandford S. A., Schmitz S., Schoonjans T., Schreiber K., Silversmit G., Srama R., Stephan T., Sterken V. J., Stroud R. M., Sutton S., Trieloff , M. , Tsou P., Tsuchiyama A., Tyliszczak T., Vekemans B., Vincze L., Korff J. V., Wordsworth N., Zevin D., Zolensky M. E., and >30,000 Stardust@home dusters. 2014. Stardust Interstellar Preliminary Examination VI: Quantitative elemental analysis by synchrotron X-ray fluorescence nanoimaging of eight impact features in aerogel. *Meteoritics & Planetary Science*, doi:10.1111/maps.12208.

Sterken V. J., Westphal A. J., Altobelli N., Grün E., Hillier J. K., Postberg F., Srama R., Allen C., Anderson D., Ansari A., Bajt S., Bastien R. S., Bassim N., Bechtel H. A., Borg J., Brenker F. E., Bridges J., Brownlee D. E., Burchell M., Burghammer M., Butterworth A. L., Changela H., Cloetens P., Davis A. M., Doll R., Floss C., Flynn G., Frank D., Gainsforth Z., Heck P. R., Hoppe P., Hudson B., Huth J., Hvide B., Kearsley A., King A. J., Lai B., Leitner J., Lemelle L., Leroux H., Leonard A., Lettieri R., Marchant W., Nittler L. R., Ogliore R., Ong W. J., Price M. C., Sandford S. A., Tresseras J. S., Schmitz S., Schoonjans T., Silversmit G., Simionovici A., Solé V. A., Stephan T., Stodolna J., Stroud R. M., Sutton S., Trieloff M., Tsou P., Tsuchiyama A., Tyliszczak T., Vekemans B., Vincze L., Korff J. V., Wordsworth N., Zevin D., Zolensky M. E., and >30,000 Stardust@home dusters. 2014. Stardust Interstellar Preliminary Examination X: Impact speeds and directions of interstellar grains on the Stardust dust collector. *Meteoritics & Planetary Science*, doi:10.1111/maps.12219.

Stroud R. M., Allen C., Anderson D., Ansari A., Bajt S., Bassim N., Bastien R. S., Bechtel H. A., Borg J., Brenker F. E., Bridges J., Brownlee D. E., Burchell M., Burghammer M., Butterworth A. L., Changela H., Cloetens P., Davis A. M., Doll R., Floss C., Flynn G., Frank D. R., Gainsforth Z., Grün E., Heck P. R., Hillier J. K., Hoppe P., Huth J., Hvide B., Kearsley A., King A. J., Lai B., Leitner J., Lemelle L., Leroux H., Leonard A., Lettieri R., Marchant W., Nittler L. R., Ogliore R., Ong W. J., Postberg F., Price M. C., Sandford S. A., Sans Tresseras J., Schmitz S., Schoonjans T., Silversmit G., Simionovici A. S., Solé V. A., Srama R., Stephan T., Sterken V. J., Stodolna J., Sutton S., Trieloff M., Tsou P., Tsuchiyama A., Tyliszczak T., Vekemans B., Vincze L., Korff J. V., Westphal A. J., and Zevin D. 2014. Stardust Preliminary Examination XI: Identification and elemental analysis of impact craters on Al foils from the Stardust Interstellar Dust Collector. *Meteoritics & Planetary Science*, doi:10.1111/maps.12136.

Tsou P., Brownlee D. E., Sandford S. A., Horz F., and Zolensky M. E. 2003. Wild 2 and interstellar sample collection and Earth return. *Journal of Geophysical Research* 108:8113.

Westphal A. J., Snead C., Butterworth A., Graham G. A., Bradley J. P., Bajt S., Grant P. G., Bench G., Brennan S., and Pianetta P. 2004. Aerogel keystones: Extraction of complete hypervelocity impact events from aerogel collectors. *Meteoritics & Planetary Science* 39:1375–1386.

Westphal A. J., Anderson D., Butterworth A. L., Frank D. R., Hudson B., Lettieri R., Marchant W., Korff J. V., Zevin D., Ardizzone A., Campanile A., Capraro M., Courtney K., Crumpler D., Cwik R., Gray F. J., Imada G., Karr , J. , Lau Wan Wah L., Mazzucato M., Motta P. G., Spencer R. C., Woodrough S. B., Santoni I. C., Sperry G., Terry J., Wordsworth N., Yanke T. Sr., Allen C., Ansari A., Bajt S., Bastien R. S., Bassim N., Bechtel H. A., Borg J., Brenker F. E., Bridges J., Brownlee D. E., Burchell M., Burghammer M., Changela H., Cloetens P., Davis A. M., Doll R., Floss C., Flynn G., Gainsforth Z., Grün E., Heck P. R., Hillier J. K., Hoppe P., Huth J., Hvide B., Kearsley A., King A. J., Lai B., Leitner J., Lemelle L., Leroux H., Leonard A., Nittler L. R., Ogliore R., Ong W. J., Postberg F., Price M. C., Sandford S. A., Tresseras J. S., Schmitz S., Schoonjans T., Silversmit G., Simionovici A. S., Solé V. A., Srama R., Stephan T., Sterken V. J., Stodolna J., Stroud R. M., Sutton S., Trieloff M., Tsou P., Tsuchiyama A., Tyliszczak T., Vekemans B., Vincze L., Zolensky M. E., and > 30,000 Stardust@home dusters. 2014a. Stardust Interstellar Preliminary Examination I: Identification of tracks in aerogel. *Meteoritics & Planetary Science*, doi:10.1111/maps.12168.

Westphal A. J., Bechtel F. A., Brenker F. E., Butterworth A. L., Flynn G., Frank D. R., Gainsforth Z., Hillier J. K., Postberg F., Simionovici A. S., Sterken V. J., Stroud R. M., Allen C., Anderson D., Ansari A., Bajt S., Bastien R. S., Bassim N., Borg J., Bridges J., Brownlee D. E., Burchell M., Burghammer M., Changela H., Cloetens P., Davis A. M., Doll R., Floss C., Grün E., Heck P. R., Hoppe P., Hudson B., Huth J., Hvide B., Kearsley A., King A. J., Lai B., Leitner J., Lemelle L., Leroux H., Leonard A., Lettieri R., Marchant W., Nittler L. R., Ogliore R., Ong W. J., Price M. C., Sandford S. A., Sans Tresseras J., Schmitz S., Schoonjans T., Silversmit G., Solé V. A., Srama R., Stephan T., Stodolna J., Sutton S., Trieloff M., Tsou P., Tsuchiyama A., Tyliszczak T., Vekemans B., Vincze L., Korff J. V., Wordsworth N., Zevin D., Zolensky M. E., and > 30,000 Stardust@home dusters. 2014b. Final reports of the Stardust Interstellar Preliminary Examination. *Meteoritics & Planetary Science*, doi:10.1111/maps.12221.

Whittet D. C. B., Boogert A. C. A., Gerakines P. A., Schutte W., Tielens A., Degraauw T., Prusti T., Vandishoeck E. F., Wesselius P. R., and Wright C. M. 1997. Infrared spectroscopy of dust in the diffuse interstellar medium toward Cygnus OB2 No. 12. *The Astrophysical Journal* 490:729–734.